



Full Length Research Article

INFLUENCE OF Cr₂O₃ ON STRUCTURAL PARAMETERS OF SCREEN PRINTED ZNO THICK FILMS

*Patil, A.V.

M.G. Vidyamandir's A.S. C. college Surgana, Nashik (M.S.), India

ARTICLE INFO

Article History:

Received 21st January, 2016
Received in revised form
19th February, 2016
Accepted 06th March, 2016
Published online 27th April, 2016

Key Words:

ZnO; Cr₂O₃,
Screen printing,
XRD,
SEM.

ABSTRACT

Thick films of pure and Cr₂O₃ doped ZnO with various concentrations (1 wt. %, 3 wt. %, 5 wt. %, 7 wt% and 10 wt%) of Cr₂O₃ were prepared on alumina substrates using a screen printing technique. These films were fired at a temperature of 700°C for two hours in an air atmosphere. Morphological, compositional and structural properties of the samples were studied using the scanning electron microscopy (SEM) and X-ray diffraction techniques respectively. Crystallite size, lattice parameters and specific surface area of undoped and doped films were determined. There is change in crystallite size, lattice parameters and specific surface area of ZnO films due to addition of Cr₂O₃.

Copyright © 2016, Patil. This is an open access article distributed under the Creative Commons Attribution License, which permits unrestricted use, distribution, and reproduction in any medium, provided the original work is properly cited.

INTRODUCTION

The ZnO is multifunctional material. Because of its high chemical stability, low dielectric constant, large electromechanical coupling coefficient and luminous transmittance, ZnO based materials have been used as dielectric ceramic, pigment, catalyst and sensing material. ZnO has hexagonal wurtzite structure, lattice parameters $a = 3.2539 \text{ \AA}$ and $c = 5.2098 \text{ \AA}$, and belongs to the space group P6₃mc (Liu *et al.*, 2001). This material stands out among the semiconductors due to its large band gap (3.37 eV) associated with a high exciton binding energy (60 meV) (Kobata *et al* 2003, Fu *et al.*, 2007). Reducing the size of the ZnO to the nanoscale changes its properties significantly, since they are dependent on the size, orientation and morphology of the particles (Duan *et al.*, 2007). This material has many technological applications such as opto-electronic devices, catalysts, cosmetics, gas sensors, varistors and pigments (Liu *et al.*, 2007, Viswanatha *et al.*, 2004, Kanade *et al.*, 2006, Duffy *et al.*, 2007). It has been found that the electrical properties of ZnO resistor depend strongly upon the type and content of additives especially metal oxides.

Incorporation of oxides causes atomic defects to form at the grain and grain boundary, with donor or donor like defects dominating the depletion layer and acceptor and acceptor like defects dominating the grain boundary states. Since the electrical properties of ZnO varistors have been attributed to their grain boundary barriers, the effect of additives must be related to the changes they cause in the grain boundary barriers. The non-ohmic property of ZnO varistors is largely affected by the addition of metal oxides (Kusy *et al.*, 1983, Koumoto *et al.*, 1982). A growing number of different ceramic materials are used today for gas/humidity sensing. The primary mechanism associated with their potential use involves several microstructure parameters that influence sensing behavior (Fagan *et al.*, 1993).

Among them, small grain size plays an important role since it was shown that decrease of the grain size to the nanometer level leads to many interesting and new properties (Jiao *et al.*, 2002, Binks *et al.*, 1996). Additionally, when oxides with a spinel structure are considered, the determination of the cation distribution and site occupancy, defect concentration and non-stoichiometry are of considerable relevance for understanding how a ceramic material interacts with its environment (Pokhrel *et al.*, 2003; Ferreira *et al.*, 2003, Mancic *et al.*, 2004). It is already established that some spinels have advanced gas sensing and catalytic properties. The spinels such as ZnCr₂O₄ are very suitable for aggressive environments (Shimizu *et al* 1990; Honeybourne *et al.*, 1996). Catalyst prepared by various

*Corresponding author: Patil, A.V.,
M.G. Vidyamandir's A. s. C. college Surgana, Nashik (M.S.), India.

methods, and concluded that any ZnO–Cr₂O₃ mixed catalyst is composed of two phases, i.e. ZnO and ZnCr₂O₄, and presents higher resistance to the aging of catalyst than non-promoted ZnO catalyst, and that promoting action is mainly due to the hindering action of the promoter, Cr₂O₃ upon the recrystallization of ZnO (Matsui Toshiji, 1956). ZnO promoted with Cr₂O₃ possesses improved catalytic activity for the synthesis reaction and also has a better sulphur tolerance (Naidu *et al.*, 1973). A small additive of Cr₂O₃ increases the electric breakdown by decreasing the grain size (Skidan, 2003). This paper deals with the explanation of structural performance of ZnO: Cr₂O₃ thick films prepared by screen printing technique.

MATERIALS AND METHODS

The alumina substrates used for deposition of thick film resistors using screen printing technique were cleaned initially by using soap solution. Further, they were cleaned by using the chromic acid to remove the finger prints and other impurities present on the substrates. Finally, all the substrates were washed by distilled water several times and then with acetone. Lastly, the substrates were dried under the IR lamp. Cr₂O₃ was used as an additive. The ZnO: Cr₂O₃ pastes used in screen printing were prepared by maintaining the inorganic to organic materials ratio of 70:30. Inorganic part consists of a functional material (Analar grade ZnO powder calcined at 400 °C for 2 h in a muffle furnace), additive (Cr₂O₃) and glass frit (70 wt. % PbO, 18 wt. % Al₂O₃, 9 wt. % SiO₂ and 3wt. % B₂O₃). Organic parts consist of 8% ethyl cellulose (EC) and 92% butyl carbitol acetate (BCA). The Analar (AR) grade ZnO with x wt. % Cr₂O₃ (x = 1, 3, 5, 7 and 10%) and 5 wt. % of glass frit were mixed thoroughly in an acetone medium with mortar and pestle. A solution of EC and BCA in the ratio 8:92 was made, which was added drop by drop until proper thixotropic properties of the paste were achieved. ZnO thick films were prepared on alumina substrates using a standard screen-printing technique. A nylon screen (mesh no.140) was used for screen-printing.

The required mask (2 x 1.25 cm) was developed on the screen using a standard photolithography process. The paste was printed on clean alumina substrates (5 x 2 cm) with the help of a mask. The pattern was allowed to settle for 15 to 20 minutes in air. The films were dried under infrared radiation for 45 minutes to remove the organic vehicle and then fired at a temperature of 700°C for 2 h (which includes the time required to achieve the peak firing temperature , constant firing for 30 minutes at the peak temperature and then to attain the room temperature) in a muffle furnace. During the firing process glass frit melted and the functional material and additive were sintered. The function of glass frit is to bind the grains of functional and additive materials together and also to adhere the film firmly to the substrate surface. The structural properties of ZnO: Cr₂O₃ films were investigated using X-ray diffraction analysis from 20–80° (Rigaku diffract meter (Miniflex Model, Rigaku, (Japan) with CuK α , $\lambda=0.1542$ nm radiation) with a 0.1°/step (2 θ) at the rate of 2 s/step. A scanning electron microscopy (SEM- JOEL JED-2300) was employed to characterize the surface morphology. The composition of ZnO thick film samples were analyzed by an energy dispersive X- ray spectrometer (JOEL-JED 6360 LA).

The crystallite size (D) was estimated by using the Debye Scherrer formula (Patil 2016),

$$D = \frac{0.9\lambda}{\beta \cos\theta} \quad (1)$$

where, β = Full angular width of diffraction peak at the at half maxima peak intensity, λ = wavelength of X-ray radiation. From the XRD pattern, the lattice constants of ZnO phase in all doping concentrations can be calculated using the equation (Patil 2016),

$$\frac{1}{d^2_{101}} = \frac{4}{3} \left(\frac{1}{a^2} \right) + \frac{1}{c^2} \quad (2)$$

where 'd' is interplanar distance, 'a' and 'c' are lattice constants (being hexagonal structure, $\frac{c}{a} = \sqrt{\frac{8}{3}}$).

Also the lattice constant of observed cubic spinel phase ZnCr₂O₄ in all added concentrations of Cr₂O₃ can be calculated using the equation (Patil 2016),

$$d_{311} = \frac{a}{\sqrt{h^2 + k^2 + l^2}} \quad (3)$$

where 'd' is interplanar distance and 'a' is lattice constant (being cubic structure a=b=c).

From the SEM photographs, the specific surface area was calculated for spherical particles using the following equation (Patil 2016),

$$S_w = \frac{6}{\rho d} \quad (4)$$

where d is the diameter of the particles, ρ is the density of the particles.

RESULTS AND DISCUSSION

1 XRD

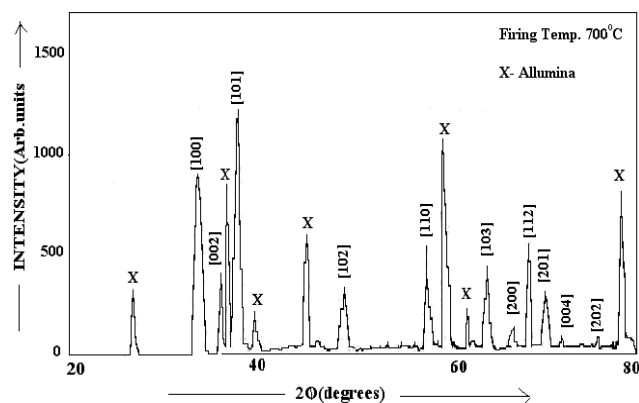


Fig. 1. XRD pattern of undoped ZnO films

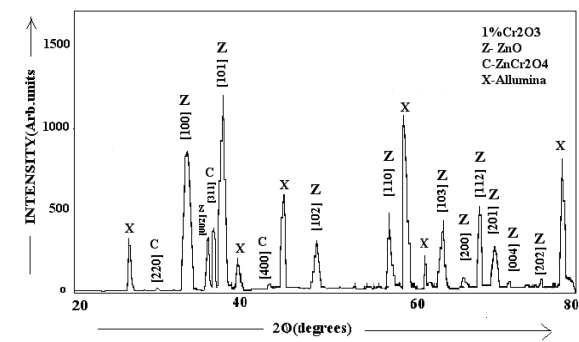
Figure 1 shows X-ray diffraction patterns obtained for ZnO thick films deposited on alumina substrates and fired at 700°C. The observed diffraction peaks correspond to the hexagonal wurtzite structure of ZnO (JCPDS 36- 14510) (Brook 1991).

In addition, no diffraction peaks from Zn could be found revealing that only ZnO single phase was formed. The other peaks observed correspond to the alumina substrate. Also XRD analysis evaluates the crystallite size of the thick films. The higher peak intensities of an XRD pattern is due to the better crystallinity and bigger crystallite size can be attributed to the agglomeration of particles. It has been observed that (101) reflections are of maximum intensity, which indicates that ZnO films have preferred orientation in the (101) plane. The average crystallite size was calculated from XRD pattern using eq.1 Debye Scherer's formula and it has been observed that the crystallite size for undoped ZnO films fired at 700°C was 18.67nm. From the XRD pattern, the lattice constants of ZnO can be calculated using the equation 2, calculated values of lattice constants are given in Table 1.

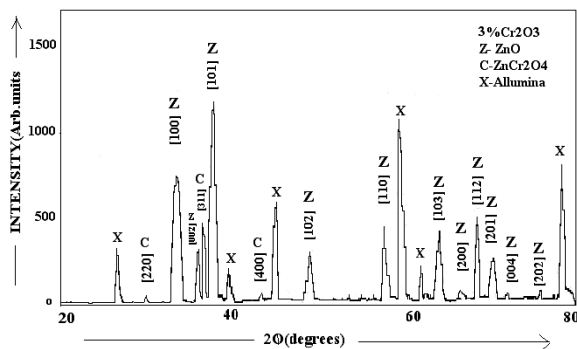
Table 1. Lattice constants of ZnO

Firing Temperature	a (Å ^o)	c (Å ^o)
700°C	3.1894	5.208

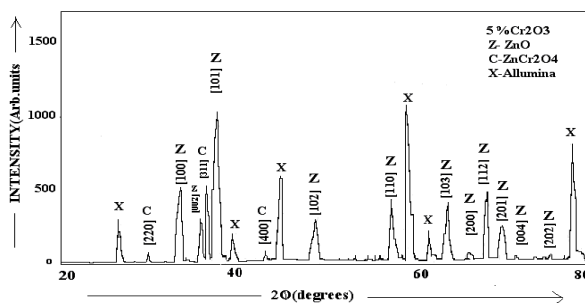
Lattice constants of ZnO are slightly depending on its stoichiometry. From Table 1, it has been observed that there is variation of lattice constants from JCPDS value (a = 3.25Å^o, c = 5.207 Å^o).



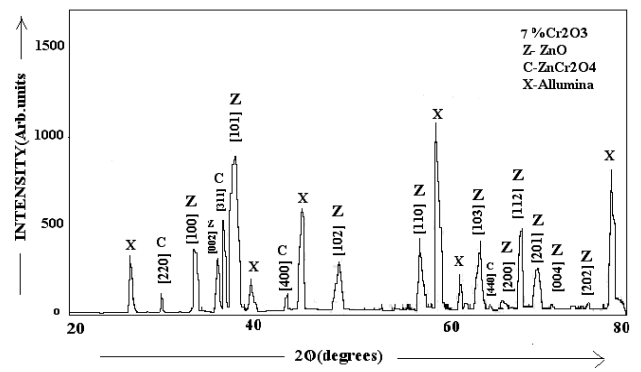
(a) 1% Cr₂O₃



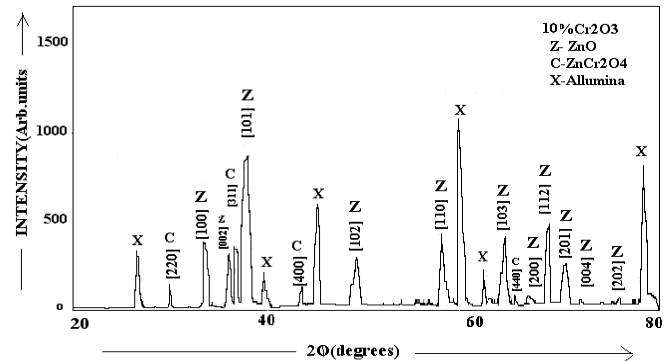
(b) 3% Cr₂O₃



(c) 5% Cr₂O₃



(d) 7% Cr₂O₃



(e) 10% Cr₂O₃

Fig.2. XRD patterns of Cr₂O₃ added ZnO films

It may be attributed due to slight variation of Zn and/or O stoichiometry in ZnO. As a semiconductor, in ZnO the radius of O²⁻ (1.32 Å^o) is larger than that of Zn²⁺ (0.74Å^o). So the variation of O content in ZnO will lead to the variation of its lattice constants, which cause the shifting of the diffraction peaks (ZnO 1992, Hai Yan Xu *et al.*, 2003). As shown in the XRD patterns for all concentrations of Cr₂O₃ added ZnO thick films, only two phases, (ZnO and ZnCr₂O₄) has been observed. There could be solid state reaction between ZnO and Cr₂O₃. This could be a result of nucleation process and the initial stage of reaction product formation, the spinel phase of ZnCr₂O₄ (Zorica *et al.*, 2002).

IRIE and SHIRAIISHI studied the effect of high temperature treatment of ZnO-Cr₂O₃ catalyst and reported as spinel formation at 700°C (Irie *et al* 1959). In ZnO thick films, ZnCr₂O₄ phase can form in the condition of a little amount of Cr₂O₃ doping. This indicates that Cr³⁺ and Zn²⁺ distribute in molecular level, and lead to the formation of ZnCr₂O₄ phase, which distributes at the grain boundaries, inhibiting the growth of ZnO grains (Jiang Sheng -Liu *et al* 2007).

Table 2. Variation of crystallite size with additive concentration of Cr₂O₃

% Additive Concentration Cr ₂ O ₃	Average crystallite size(nm)
0	18.637
1	18.637
3	18.637
5	18.637
7	17.47
10	26.13

Table 3. Lattice constants of ZnO: Cr_2O_3 films

Phase	a (\AA)	c (\AA)
ZnO	3.1894	5.208
ZnCr_2O_4	8.356	-

In all cases, the observed diffraction peaks correspond to the hexagonal wurtzite structure of ZnO (JCPDS 36-14510) and cubic spinel phase of ZnCr_2O_4 (JCPDS 22-1107). It has been observed that ZnO phase has preferred orientation in (101) plane and ZnCr_2O_4 phase has preferred orientation in (311) plane. The peak intensity of ZnO planes (101) was decreased with increase in Cr_2O_3 concentration in the films whereas peak intensity of ZnCr_2O_4 planes (311) increased up to 7% of Cr_2O_3 in the films. For the ZnO samples added with 7% and 10% Cr_2O_3 , additional peaks of very low intensities for (440) plane of ZnCr_2O_4 has been observed. For the ZnO sample added with 7% Cr_2O_3 , the preferred orientation of (311) plane of ZnCr_2O_4 phase was observed strong than other doping concentrations and slight broadening of diffraction lines of ZnO phase. Slightly broadening of diffraction lines may be attributed to small crystalline effects, crystal defects or chemical heterogeneity of the samples (Macnic *et al.*, 2003). The average crystallite size was calculated from XRD pattern using eq.1 Debye Scherer's formula and It has been observed that the crystallite size remained constant for 1%, 3%, and 5% Cr_2O_3 added ZnO samples with respect to the undoped ZnO samples, but for 7% Cr_2O_3 additive there is decrease in crystallite size. This may be attributed to the broadening of diffraction lines. Table 2 shows the variation of crystallite size with added concentration of Cr_2O_3 in ZnO samples.

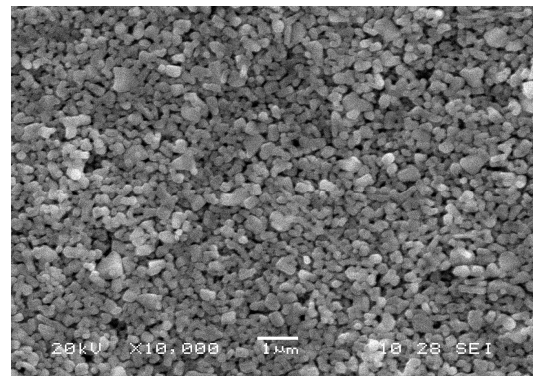
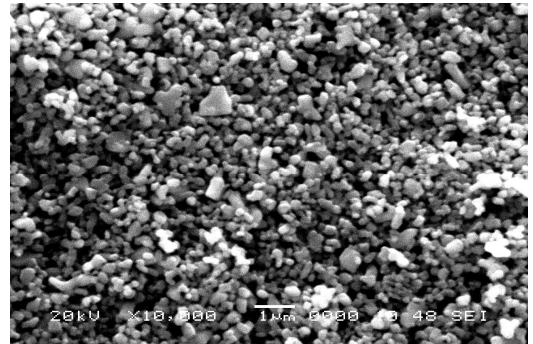
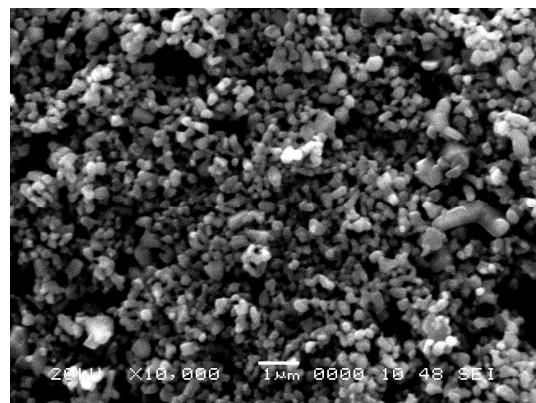
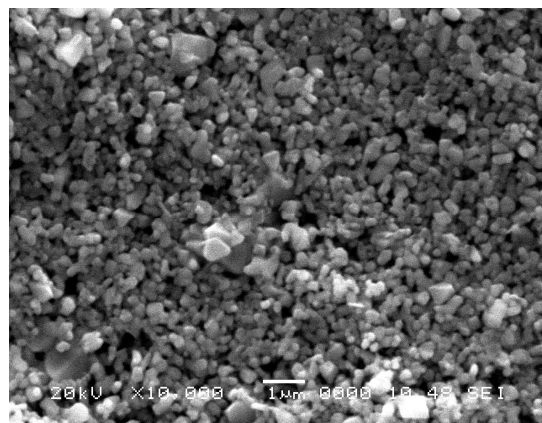
For 10% Cr_2O_3 additive, the crystallite size increases. It may be due to the agglomeration of spinel particle with ZnO particle at higher doping concentration. the lattice constant of cubic spinel phase ZnCr_2O_4 in all doping concentrations can be calculated using the equation 3. From the Table 3, it has been observed that there is variation of lattice constants from JCPDS value ($a = 3.25 \text{ \AA}$, $c = 5.207 \text{ \AA}$) of ZnO and JCPDS value ($a = 8.327 \text{ \AA}$) of ZnCr_2O_4 . The variation in lattice parameters is due to formation of non-stoichiometric and defective material (Macnic *et al.*, 2003).

SEM

Figure 3 shows SEM of undoped ZnO film fired at 700°C . Film structure is uniform and consists of a large number of spherical grains leading to a high porosity and large effective area available for the adsorption of oxygen species. The specific surface area of ZnO thick films was calculated using BET method for spherical particles using the following equation 4 and is shown in Table 4.

Table 4. Particle size and Sp. Surface area of ZnO

Firing temperature	Particle size (nm)	Specific Surface Area in m^2/g
700°C	381	2.75

**Fig. 3. SEM of ZnO thick film fired at 700°C** **(a) 1% Cr_2O_3** **(b) 3% Cr_2O_3** **(c) 5% Cr_2O_3**

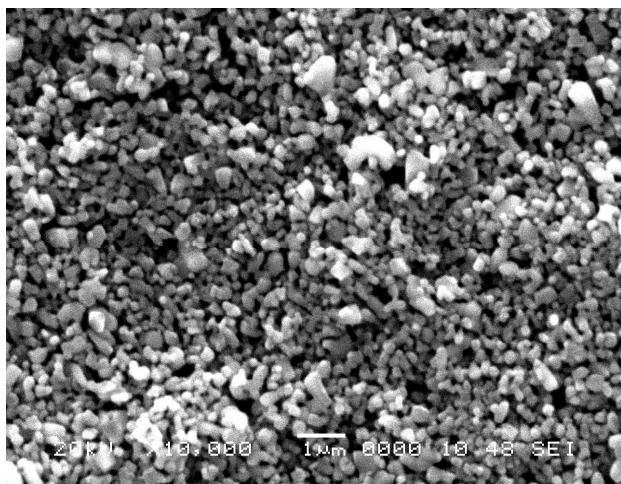
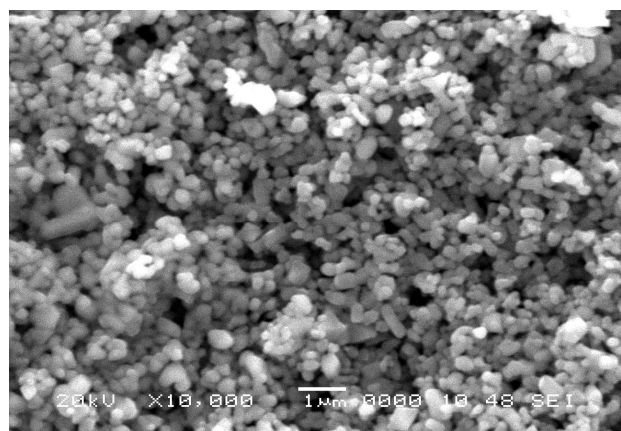
(d) 7% Cr₂O₃(e) 10% Cr₂O₃

Fig. 4. SEM of Cr₂O₃ added ZnO thick films fired at 700°C

Table 5. Variation of particle size and Sp. surface area with doping conc

wt. % of Cr ₂ O ₃	Particle size in nm	Specific Surface Area in m ² /g
1	366	2.89
3	333	3.18
5	333	3.19
7	266	4.00
10	423	2.46

The surface morphology of ZnO: Cr₂O₃ thick films were studied by characterizing the films using scanning electron microscopy. A scanning electron microscope, SEM (Model JOEL 6300(LA) Germany) was employed to characterize the samples. For SEM, all ZnO: Cr₂O₃ samples were coated with a very thin conducting gold layer (few 100Å) using vacuum evaporation/sputtering technique to avoid charging of the samples.

Figure 4.2(a, b, c, d and e) shows the SEM micrographs of ZnO: Cr₂O₃ thick films fired at 700°C. All the SEM images are recorded at 10000X magnification for comparison. The doping of Cr₂O₃ influence microstructure of the ZnO is well evinced by the formation of precipitates smaller than undoped ZnO. These precipitates are localized at the grain boundaries or in the ZnO grains and correspond to spinel phase. When

lower doping concentration is used, the particle becomes greater and more gaps are formed between them with no substantial change in the pattern. As shown in Figure 4.2 (a, b, c), there is no considerable change in the microstructure due to low doping. The particles of different size and shape are randomly distributed with voids. Some larger spinel particles distributed around the smaller functional particles. Figure 4.2(d) for 7wt. % additive showed that Cr₂O₃ grains may reside in the intergranular regions of ZnO. ZnCr₂O₄ exist between ZnO and Cr₂O₃ phase can stabilize surface zinc active sites and promote the increase in the effective surface area (Yoshisada *et al.*, 1959, Patil *et al* 2007). Figure 4.2 (e) for 10wt. % additive showed that there is agglomeration of the particles. ZnCr₂O₄ crystallites are sintered into massive particles and disposed randomly. So the particle size increases that decreases the effective surface area. From the SEM images, specific surface area can be determined. A high surface area facilitates the chemisorptions process by increasing the adsorption and desorption rates (Krupriyanov, 1996). The specific surface area of ZnO thick films was calculated using BET method for spherical particles using the following equation (Gao *et al.*, 2000). Table 5 shows the change in particle and Sp.surface area of ZnO: Cr₂O₃ thick films with doping concentration.

Conclusion

It has been possible to prepare the thick films of ZnO with Cr₂O₃ as additive by screen printing. There is change in crystallite size, lattice parameters and specific surface area of ZnO films due to addition of Cr₂O₃. The variation in lattice parameters may be due to formation of non-stoichiometric and defective material.

Acknowledgment

Author is thankful to the Management of M.G. Vidyamandir and staff of A.S.C. college, Surgana (Nashik)

REFERENCES

- Binks, D.J., Grimes, R.W., Rohl, A.L. and Gay, D.H. 1996. Morphology and structure of ZnCr₂O₄ spinel crystalli. *Journal of Materials Science*, 31 (5) 1151-1156
- Brook, R.J. 1992. Concise Encyclopedia of Advanced Ceramic Materials, the MIT Press, Massachusetts, USA.1991 JCPDS ZnO, 5 – 0664
- Duan, J.X., Wang, H. and Huang, X.T. 2007. "Synthesis and characterization of ZnO ellipsoid-like nanostructures". *Chinese Journal of Chemical Physics*, 20:613-618.
- Duffy, G.M., Pillai, S.C. and McCormack, D.E. 2007. A novel processing route for the production of nanoparticulate zinc oxide using an isophthalate precursor. *Smart Materials and Structures*. 16:1379-1381
- Fagan, J.G. and Amarakoon, V.W. 1993. "Reliability and reproducibility of ceramic sensors: Part. III. Humidity Sensors". *Am. Ceram. Soc. Bull.*, 72 (3) 119 -130
- Ferreira, T.A.S. Waerenbourgh, J.C., Mendonca, M.H.R.M.m Nunes, M.R. and Costa, F.M. 2003. "Structural and morphological characterization of FeCo₂O₄ and CoFe₂O₄ spinels prepared by a co precipitation method". *Solid State Sciences*, 5 383 – 392

- Fu, Y.S., Du, X.W., Sun, J., Song, Y.F. and Liu, J. 2007. "Single-crystal ZnO cup based on hydrothermal decomposition route". *Journal of Physical Chemistry*. 111:3863-3867.
- Gao, L., Li, Q., Song, Z., Wang, 2000. "Preparation of Nano-scale Titania Thick Film and Its Oxygen Sensitivity" *Sensors and Actuators B71*: 179-183.
- Hai Yan Xu, Hao Wang, Yong cai Zhang, Shu Wang, Mankang Zhu, Hui Yarn, 2003. "Asymmetric twinning crystals of Zinc oxide formed in a hydrothermal process". *Crystal. Res. Technol.*, 38 (2003) 429 -432
- Honeybourne, L. C. and R. K. Rasheed. 1996. "Nitrogen dioxide and volatile sulfide sensing properties of copper, zinc and nickel chromite", *J. Mater. Chem.*, 6 (3): 277 – 283
- Irie, T., Shiraishi, T., 1959. "Stoichiometric modifications of ZnO-Cr₂O₃ catalyst system in oxidizing and reducing atmospheres" *Nippon Kagaku Zasshi, (Journal of the Chemical Society of Japan Pure Chemistry)* 80: 107-131
- Jiang Sheng-lin, Zhang Hai-bo, Xie Tian-tian, Fan Mao-yan, Zeng Yi-ke, Lu Wen-Zhong, 2007. "Effect of Cr doping on secondary phases and electrical properties of zinc oxide ceramic thick film varistors", *Trans. Nonferrous Met. Soc. China*, 17: 794-797
- Jiao, Z., Ye, G., Chen, F., Li, M. and Liu, J. 2002. "The Kanade, K.G., Kale, B.B., Aiyer, R.C. and Das, B.K. 2006. Effect of solvents on the synthesis of nano-size zinc oxide and its properties. *Materials Research Bulletin*. 41:590-600.
- Koumoto, K., Aoki, K. and Kitaori, N. 1982. "Enhancement of electrical conduction in ZnO by CoO doping" *Comm. Am. Ceram. Soc.*, 65 C 93-C 94
- Kubota, J., Haga, K., Kashiwaba, Y., Watanabe, H., Zhang, B.P. and Segawa, Y. 2003. "Characteristics of ZnO whiskers prepared from organic zinc." *Applied Surface Science*. 216:431-435.
- Kupriyanov, L.Y. 1996. *Semiconductor Sensors in Physico-Chemical Studies: Handbook of Sensors and Actuators 4*. Elsevier, Amsterdam 1996. Kress-Rogers, E. (ed.):P412
- Kusy A, T. G. M. Kleinpenning 1983. "Conduction mechanism and 1/f noise in ZnO varistors", *J. Appl. Phys.*, 54 2900-2906
- Liu, R., Vertegel, A.A., Bohannan, E.W., Sorenson, T.A. and Switzer, J.A. 2001. "Epitaxial electrodeposition of zinc oxide nanopillars on single-crystal gold" *Chemistry of Materials*. 13:508-512.
- Liu, Y., Zhou, J., Larbot, A. and Persin, M. 2007. "Preparation and characterization of nano-zinc oxide." *Journal of Materials Processing Technology*, 189:379- 383
- Mancic, L., Marinkovic, Z., Vulic, P. and Milosevic, O. 2004. "The Synthesis – Structure Relationship in the ZnO-Cr₂O₃ system" *Science of Sintering*, 36 189-196
- Mancic, L., Marinkovic, Z., Vulic, P. Moral, C. and Milosevic, O. 2003. "Morphology, structure and nonstoichiometry of ZnCr₂O₄ nanophased powder" *Sensor 3*: 415-423
- Matsui Toshiji, 1956. "Investigation of ZnO-Cr₂O₃ Mixed Catalyst by Electron Microscope and selected-area Electron diffraction" *Journal of the research institute for catalysis, Hokkaido University* 4(2): 109-131
- Naidu, S. R., A. K. Banerjee, N. C. Ganguli, S. P. Sen, 1973. "Stoichiometric modifications of ZnO-Cr₂O₃ Catalyst system in oxidizing and reducing atmospheres" *Journal of The Research Institute for Catalysis, Hokkaido Univ.* 21(3): 172 - 186
- Patil, A.V. 2016. "Effect of Nb₂O₅ as an additive on structural parameters of ZnO thick film, *International Journal of Latest Research in Science and Technology* 5(1) : 102-106
- Patil, D. R., L. A. Patil, P. P. Patil, 2007. "Cr₂O₃- activated ZnO thick film resistors for ammonia gas sensing operable at room temperature" *Sensors and Actuators B* 126(2): 368-374
- Pokhrel, S., Jeyaraj, B. and Nagaraja, K.S. 2003. "Humidity-sensing properties of ZnCr₂O₄-ZnO composites", *Mater. Lett.* 57 (22) 3543 -3548
- preparation of ZnGa₂O₄ nanocrystals by spray co precipitation and its gas sensing characteristics" *Sensors* 2(3) 71-78
- Shimizu, Y., Kusano, S. 1990. "Oxygen-sensing properties of spinel-type oxides for stoichiometric air/fuel combustion control", *J. Am. Ceram. Soc.* 73 818-824
- Skidan, B. K. 2003. The Effect of Additives on properties of Ceramics Based on Zinc Oxides. *Glass and Ceramics*, 60(9-10) :339-341
- Viswanatha, R., Sapra, S., Satpati, B., Satyam, P.V., Dev, B.N. and Sarma, D.D. 2004. Understanding the quantum size effects in ZnO nanocrystals. *Journal of Materials Chemistry*, 14:661-668.
- Yoshisada Ogino, Masaaki Oba, Hirishi Uchida, 1959 "Study on Zinc Oxide-Chromium Oxide Catalyst.IV. Dependency of Catalytic Activity on Catalyst structure", *Bull. of the Chem. Soc. of Japan*, 32(6) (1959) 616- 621
- Zorica V. Marinkovic, Tatjana V. Sreckovic, Ireana Petrovic Pelevic and Momcilo M. Ristic, 2002. "Structural Changes of ZnO - Cr₂O₃ System during Mechanical Activation and Their Influence on the Spinel Synthesis" *Chemistry for Sustainable Development* 1-2: 113-118
